Enhancing the Vertical Resolution of Coherent Optical Receivers

Fabio A. Barbosa, *Member, IEEE,* Filipe M. Ferreira, *Senior Member, IEEE*

***Abstract*— The constantly increasing capacity demand in optical fiber transmission systems has driven the development of higher-order modulation to share the cost and power-consumption of optoelectronic components across many bits. However, higher-order modulation imposes challenging requirements on high-speed optoelectronic transceiver components such as on the vertical resolution of analog-to-digital and digital-to-analog converters. State-of-the-art high-speed converters limit the development of next-generation systems above 6 bit/s/Hz/pol at symbol rates beyond 100 Gbaud for Nyquist shaped channels. Ultimately, in the absence of fiber nonlinearity the upper limit on the available signal-to-noise ratio is bounded by the transceiver subsystems. Here we propose a novel optoelectronic technique to enhance the effective vertical resolution of coherent receivers through optical intensity reshaping. Finally, we show that the proposed technique to increase the effective resolution will also boost the performance of digital backpropagation used to mitigate fiber Kerr nonlinear response.**

***Index Terms*—optical communications, coherent detection, digital-to-analog converter, analog-to-digital converter, effective number of bits**

I. Introduction

STATE-of-the-art high-speed complementary metal-oxide-semiconductor (CMOS) analog-to-digital converters (ADCs) and digital-to-analog converters (DACs) reach noise floors of around 5 effective number of bits (ENoB) for ultra-high-speed sampling rates at ~100 GS/s [1-4]. Presently, ADC/DAC technology is being pushed to the limit to deliver 64-QAM, with higher-order formats requiring adding ~1 effective bit for each extra bit-per-symbol to get to the same implementation penalty [5, 6]. This could remain the case for the near future as the improvement of ultra-high-speed pure CMOS converters is saturating [4]. Meanwhile, higher-order constellations are being considered [7] and, in many cases, in combination with constellation shaping techniques (probabilistic and/or geometric shaping) [8-10].

The performance of converters is dominated by clock jitter at higher frequencies [1]. For example, aperture jitter is the inability of ADCs to sample at precisely defined time instants. The signal-to-noise-plus-distortion ratio (SNDR) in decibel is related to aperture jitter as $\mathrm{SNDR[dB]} = -20\log10(2\pi f t_j)$ where f is the input analog frequency and t_j is the rms aperture jitter of the ADC – assuming an infinite resolution ADC. Then, theoretical ENoB can be calculated noting that ENoB[bits] = (SNDR[dB]-1.76)/6.02 [11]. In this way, for a given aperture jitter, it can be understood that the theoretical *analog bandwidth is halved for each extra effective bit*. Reversely, if the required ENoB is reduced by one bit the theoretical analog bandwidth can be doubled, which would allow to increase the bit rate and reduce the cost and energy consumption per bit. This paper mainly contributes with techniques to achieve the latter, reducing the ENoB requirements allowing for a wider analog bandwidth.

Without a breakthrough on ADCs/DACs technology we are approaching a regime of diminishing returns for *single optical head receivers*. Here we argue that in coherent transceivers technology we could take a transformative leap towards parallel processing similar to that in microprocessors [12], to ensure performance scaling at a sustainable cost and energy consumption. We explore a solution to improve the performance of *optical coherent transceivers* using optical intensity reshaping to improve the overall vertical resolution. We will be focusing only on the coherent receiver side in this paper.

In conventional coherent optical systems, the incoming signal is mixed with a local oscillator (LO) laser in such a way (see Fig. 1) that, through balanced detection plus ADC and digital signal processing (DSP), the amplitude, phase and polarization of the transmitted signal can be retrieved. In this way, current metro and long-haul systems maximize throughput by simultaneously using quadrature-amplitude modulation (QAM) and polarization multiplexing (PM): with spectral efficiency increasing with constellation cardinality but limited by the available vertical resolution in DACs and ADCs [13]. Fig. 2 (a) shows a high-order constellation, 64-QAM. It can be seen that a nonconstant envelope signal leads to a significant peak-to-average power ratio (PAPR), which in turn significantly decreases the effective dynamic range of ADCs and so the achievable signal-to-noise ratio (SNR) at the receiver [14]. Being so critical, to maximize the dynamic range in practical coherent receivers the gain of the transimpedance amplifiers seating in front of the ADCs are constantly adapted (on a µs-to-

Submitted to IEEE/Optica Journal of Lightwave Technology on September 28th. This work was supported by the UKRI Future Leaders Fellowship MR/T041218/1 and MR/Y034260/1. To access the underlying data for this publication, see: doi.org/10.5522/04/24211254. F. A. Barbosa and F. M. Ferreira declare a relevant patent application: United Kingdom Patent Application No. 2411510.7.

F. A. Barbosa and F. M. Ferreira are with the Department of Electronic and Electrical Engineering at University College London, UK (email: fabio.barbosa@ucl.ac.uk; f.ferreira@ucl.ac.uk). Color versions of one or more figures in this article are available at https://doi.org/xxxx. Digital Object Identifier xxxx.

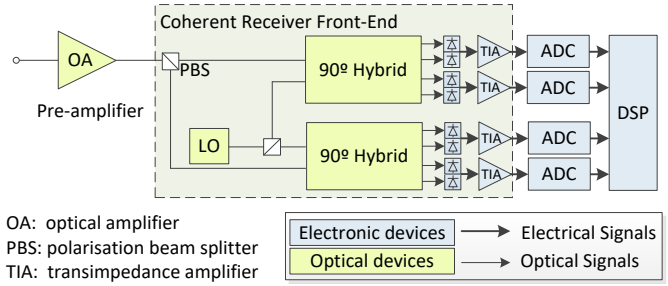

Fig. 1. Basic system concept of a conventional coherent receiver.

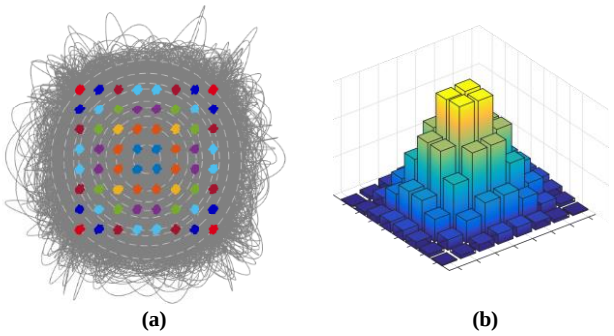

Fig. 2. a) 64-QAM (before matched filtering). b) probabilistically shaped 64-QAM with an entropy rate of 4 bits/symbol.

ms basis) to strike optimum in the trade-off between quantization noise and signal clipping noise. Furthermore, a high PAPR significantly enhances Kerr induced signal distortion and can severely reduce system reach [15]. To suppress the nonlinear distortion, digital nonlinear compensation techniques, such as digital backpropagation (DBP) [16, 17], have been applied with some success (0.1-2 dB improvement). However, their performance is limited by the ENoB of the receiver [14].

Constellation shaping techniques, such as probabilistic and geometric shaping, have been recently used to improve throughput by tailoring high-order constellations to the nonlinear fiber channel [9], but also to serve as a platform for rate adaptation [18-20]. Probabilistic shaping is characterized by modifying the probability of occurrence of constellation symbols, prioritizing those from inner rings [9] as shown in Fig. 2 (b). This process is sometimes done in a sacrificial way with sporadic symbols in the outer rings used to sunk nonlinear distortion away from the main payload [21]. The impact of ENoB in probabilistically shaped constellations has been investigated in [22, 23], where it is shown that high-order shaped constellations can be more susceptible to SNR penalties at reduced ENoB. Throughout this paper, we will only consider conventional QAM constellations while ENoB gains discussed here can also be translated to systems using constellation shaping techniques.

Here we explore an optical processing technique to improve the ENoB at coherent receivers which will not only boost the receiver sensitivity, but also the performance of digital nonlinear compensation techniques, such as DBP [16, 17]. Instead of additional electronic processing, we will be using optical signal and optoelectronic processing as it delivers broadband signal processing with high energy efficiency and ultra-low-noise [24]. The remainder of this paper is organized as follows. Section II presents in detail the techniques proposed here to enhance the vertical resolution of coherent receivers. Section III introduces the transmission setup used to investigate by simulations the proposed techniques. Section IV analyzes the results obtained in both the linear and nonlinear regimes when using the proposed techniques. Finally, Section V provides conclusions.

II. Proposed Methods

The method proposed here aims at improving the ENoB at coherent receivers by reducing the penalty driven by the signal PAPR through optical processing. The work in [6] identifies a relationship between ENoB and PAPR assuming that, to first order, the signal distortion (e.g., harmonics) in SNDR is proportional to the signal power. For the case of a multi-frequency signal, an expression for the SNDR including the PAPR is presented in [6],

$$\mathrm{SNDR}'[\mathrm{dB}] = 10\log_{10}\left(\frac{\alpha \cdot \mathrm{S}}{\mathrm{N} + \alpha \cdot \mathrm{D}}\right), \quad (1)$$

where S is the power of the undistorted signal, N and D are, respectively, the power of the noise and signal distortion, and α = 2/PAPR – where PAPR for a given signal x is defined as $\mathrm{PAPR[dB]} = 10\log_{10}(\max(|x|^2)/\mathrm{E}\{|x|^2\})$, where E{.} refers to the expectation operator. Experimental investigations in [6] showed that the distortion term reduces with the increase in the signal PAPR, while the noise term remains constant, supporting the use of (1) for ENoB analysis. Note that, ENoB[bits] = (SNDR[dB] - 1.76)/6.02. Taking (1) into consideration, one can observe that the increase in the signal PAPR, for a given signal power S, leads to a reduction in the ENoB. Therefore, in the following we aim at reducing the PAPR impact.

In the following, we propose a novel approach, optical intensity reshaping (OIR) – that aims to directly reduce the PAPR of the optical signal prior to detection. Fig. 3 includes versions of OIR with and without local optical polarization splitting (OPS). These techniques would take advantage of the possibilities open by maturing photonic integrated circuits.

The OIR technique improves the performance of a single optical head coherent receiver by reshaping the intensity envelope of the incoming optical signal and removing as much intensity information as possible and so reducing the PAPR – the implementation is illustrated in Fig. 3 (a). This is done by using an intensity modulator driven by the reciprocal of the intensity waveform obtained from an optical tap using direct detection (DD) (i.e., multiplicative inverse $1/r_{\mathrm{DD}}$). The signal inversion can be done either in the analog domain using log and anti-log amplifiers, or digital signal processing (DSP) in-between a state-of-the-art ADC-DAC pair. Here we follow the latter. After reducing (ideally to 1) the PAPR of the optical signal impinging on the coherent receiver front-end, ADCs are only required to deal with residual fluctuations of the intensity

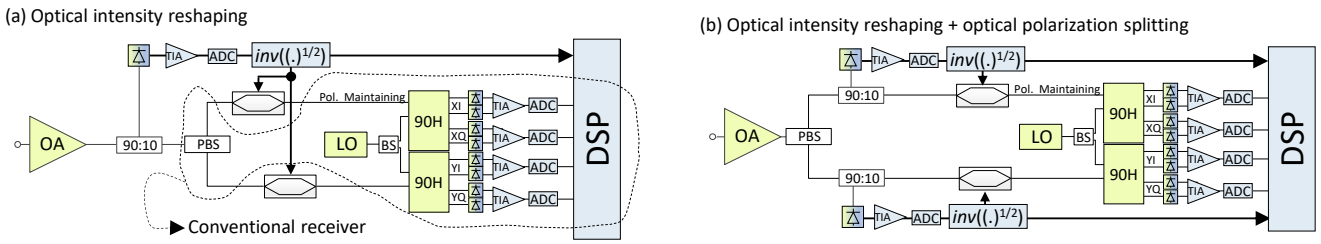

Fig. 3. Set of techniques to improve coherent detection of high PAPR optical signals: (a) optical intensity reshaping, (b) optical intensity reshaping including polarisation aware reshaping.

(a) (b)

Fig. 4. Example 64-QAM constellations (before matched filtering), same as Fig. 2(a)) after (a) OIR, (b) OIR+OPS. Colour mapping: grey points correspond to samples between symbols and colours correspond to different symbols at optimum sampling time. In all cases there are 128 samples per symbol and ENoB is set to 7 bits without any jitter or bandwidth restriction.

in both quadrature components. To reconstruct the incoming optical signal the quantization levels from both stages (i.e., the optical tap plus ADC and the conventional coherent receiver front-end) are passed to the receiver DSP circuit. By passing the digitized intensity signal to the DSP, the detected field is reconstructed before the other DSP blocks (see Fig. 5).

In Section III and IV, we will be analyzing the OIR and OIR+OPS techniques in the presence of transceiver and fiber impairments, such as: laser phase noise and carrier frequency offset; DAC/ADC quantization and jitter noise as well as bandwidth limitations; and fiber polarization mode dispersion (PMD). Here, in the remaining of Section II, we analyze idealized signal constellations after applying technique OIR or OIR+OPS in the absence of any laser, fiber or ADC/DAC impairments/limitations except for quantization noise.

Fig. 4 (a) shows an idealized signal constellation after applying *technique OIR* to a 64-QAM constellation using an idealized ADC with ENoB = 7 bits to discretize the optical tap DD signal. The outer symbol transitions are partially suppressed. However, it can also be seen that the constellation has not collapsed into a ring (i.e., constant amplitude signal constellation). This is because DD in the optical tap branch is polarization insensitive. To achieve further intensity stripping each polarization must be processed independently through optical polarization splitting (OPS) as shown in Fig. 3 (b). From Fig. 4(b), it can be seen that the constellation collapses into one ring, except for some minor deviations due to the limited ENoB (7 bits) of the ADC in the optical tap path. Nonetheless, this is an idealized case without laser phase noise, carrier frequency offset, PMD, or ENoB frequency limitations.

Note that similar improvements to those introduced by OPS can be obtained by splitting the *local* phase quadrature components. However this would not be trivial and it could require using a nonlinear parametric process of the likes of a phase sensitive amplifier (PSA) [25].

From the diagrams in Fig. 3(a) and Fig. 3(b), one can expect additional insertion losses. These can be minimized when adding the additional opto-electronic components in Fig. 3 to an existing transceiver photonic integrated circuit (PIC) (such that additional fibre-chip-fibre losses are avoided). In this case, the on-chip losses can be as low as 2 dB [26], more significant are the modulation loss [27] required to handle the PAPR of the driving signal which can be as large as 10 dB – see Section IV – in this way, the insertion loss of the MZMs required for OIR is considered to be 12 dB. To overcome these losses a semiconductor optical amplifier (SOA) can be integrated before the intensity modulator added by the proposed technique OIR – in this way, and for a multi-span link, the total noise figure degradation is not significant ($\lesssim$1 dB). The latest commercial transceivers already use PICs, and these integrate the transmitter modulator assembly, the integrated 90° hybrid, photodetectors, and SOAs.

III. Transmission Setup and DSP

Along this study we consider a wavelength division multiplexing (WDM) system with 5 channels, each modulated with 28 Gbaud dual-polarization 1024-QAM, spaced of 29 GHz. The simulation setup is shown in Fig 5.

To implement the techniques OIR, the ADC/DAC model proposed in [28, 29] is followed here to account for ENoB frequency dependency, including sampling jitter. According to this method the timing jitter is introduced by taking the derivative of the input signal and multiplying it with the target timing jitter before adding it back to the signal. This approach is supported by experimental validation in [28, 29] with good agreement. For the ADC model the following parameters are used as reference: $\mathrm{ENoB_{DC}}$ = 4 bits (represents the hardware bit architecture), a root mean square (RMS) jitter of 50 fs, and a 10th order Gaussian filter *with a bandwidth of half the symbol rate or a multiple for super-channel detection*. All the

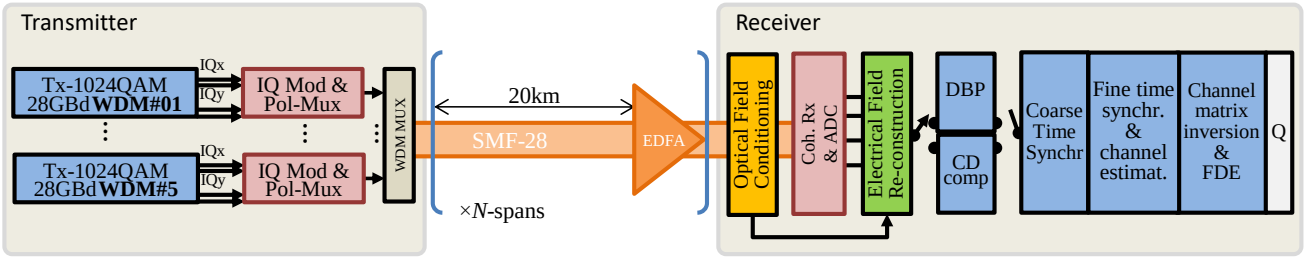

Fig. 5. Transmission simulation including optical transmitter, standard single-mode fiber, erbium doped fiber amplifier, coherent receiver, and DSP blocks.

photodiodes in the schematics of Fig. 3 have a bandwidth limitation following a 10th order Gaussian filter with a bandwidth of half the symbol rate (or a multiple in case of super-channel detection), except for the photodiode in the DD tap corresponding to the OIR case. For the latter, a raised cosine (RC) filter with a bandwidth of 0.2-times the symbol rate is applied to remove the fastest power fluctuations. Not filtering/smoothing out or attempting to re-shape these fluctuations would significantly increase the ENoB requirements at higher frequencies beyond the symbol rate.

To address the SNR degradation caused by the additional loss from the intensity modulators used exclusively in the OIR method, SOAs with a 6 dB noise figure and 12 dB gain are included prior to the modulators in the OIR configuration. This accounts for an on-chip device loss of 2 dB and a modulation loss [27] equal to the PAPR of the reshaping driving signals (for the conditions in Section IV, PAPR averages to ~10 dB, slightly lower than that of coherent optical signals due to the RC filtering applied for the DD-tap). WDM channel demultiplexing is implemented using an ideal brick-wall filter with a bandwidth equal to N_{ch} times the channel spacing, where N_{ch} is the number of WDM channels to be simultaneously detected. Furthermore, the coherent receiver simulation modules for the schemes in Fig. 3 include carrier frequency offset and laser phase noise. The impact of these impairments on the scheme proposed is analyzed in Section IV.

To recover the information signal after transmission the following DSP chain is used. For time synchronization and channel estimation, a preamble consisting of constant amplitude zero autocorrelation (CAZAC) sequences was transmitted together with the payload data. For the simulations we considered 2^{16} symbols, with a 2^{11} symbols CAZAC preamble. Root raised cosine filters with a roll-off factor of 0.01 were used for pulse shaping. The in-phase and quadrature components of each signal drove the optical field of a laser through an optical IQ modulator, and the optical signals were fed into the standard single-mode fiber (SMF) link (e.g., SMF-28 at 1550 nm). Fiber attenuation was fully compensated using an ideal erbium doped fiber amplifier with a 3 dB noise figure. After homodyne detection, the baseband electrical signals were sampled at 2 samples/symbol. Forward propagation simulation was implemented using the split-step Fourier method (SSFM) with a step bounded by the local error method [30] below 10^{-5}, and considering a PMD of 0.04 ps/√km. The other fiber parameters are: attenuation $\alpha = 0.2$ dB/km, chromatic dispersion CD = 20 ps/(nm·km), and nonlinear coefficient $\gamma = 1$ W^{-1}·km^{-1}.

As a reference, for linear compensation, the coherently received signals were ideally compensated for chromatic dispersion in the frequency domain. In all cases, PMD was subsequently compensated for using training-symbol-based channel estimation and equalization, as shown in Fig. 5. Coarse time synchronization was performed using the Schmidl & Cox autocorrelation metric. Subsequently, fine-time synchronization and channel impulse response (CIR) estimation were performed by cross-correlating with the training CAZAC sequences. The 2×2 CIR estimations were converted into the frequency domain. The multiple-input multiple-output (MIMO) frequency domain equalizer was calculated by inverting the channel matrix. Carrier frequency offset and laser phase noise compensation were performed. Then, the Q-factor for each received signal was estimated through error counting or through the mean and standard deviation of the received symbols [31] when less than 100 errors occur. The total line-rate is 2.8 Tb/s, a net-data-rate of 2.2 Tb/s given 20% FEC and 3% training sequences overheads.

For the case with nonlinear digital compensation, DBP is implemented by launching the coherently received signals into a virtual fiber with characteristics of opposite-sign values of those in the transmission channel. DBP is implemented using the SSFM with fixed step size [30].

IV. Results

Now we estimate the potential gain that the method presented in Section II can deliver. All ADCs in the proposed receivers have the same ENoB, jitter and bandwidth limitations, including the ADC following the DD optical tap. In the following, we present results for the central channel in the super-channel configuration.

A. Back-to-back configuration

For all the proposed schemes in Section III, we first evaluate the Q-factor as a function of ADCs ENoB in a back-to-back configuration loaded with chromatic dispersion and spontaneous emission noise. OSNR is set to 50 dB and dispersion is set to 17 μs/nm.

Fig. 6 analyzes the impact of characteristics of the ADC (ENoB and sampling jitter) and other impairments present in coherent receivers (time misalignment/skew, laser phase noise and frequency offset) on the recovered signal Q-factor and on the PAPR obtained when using method OIR. Assuming homodyne detection and an ideal laser, Fig. 6 (a) investigates the Q-factor for OIR with and without OPS as a function of ADCs ENoB. In overall, Q-factor improves with ENoB at a pace of 6 dB per extra bit. Note that the SNR of an ideal N-bit ADC is SNR [dB] = $6.02 \times N + 1.76$. However, as ENoB increases, the Q-factor improvement saturates as the link OSNR limits the overall performance and quantization noise is no

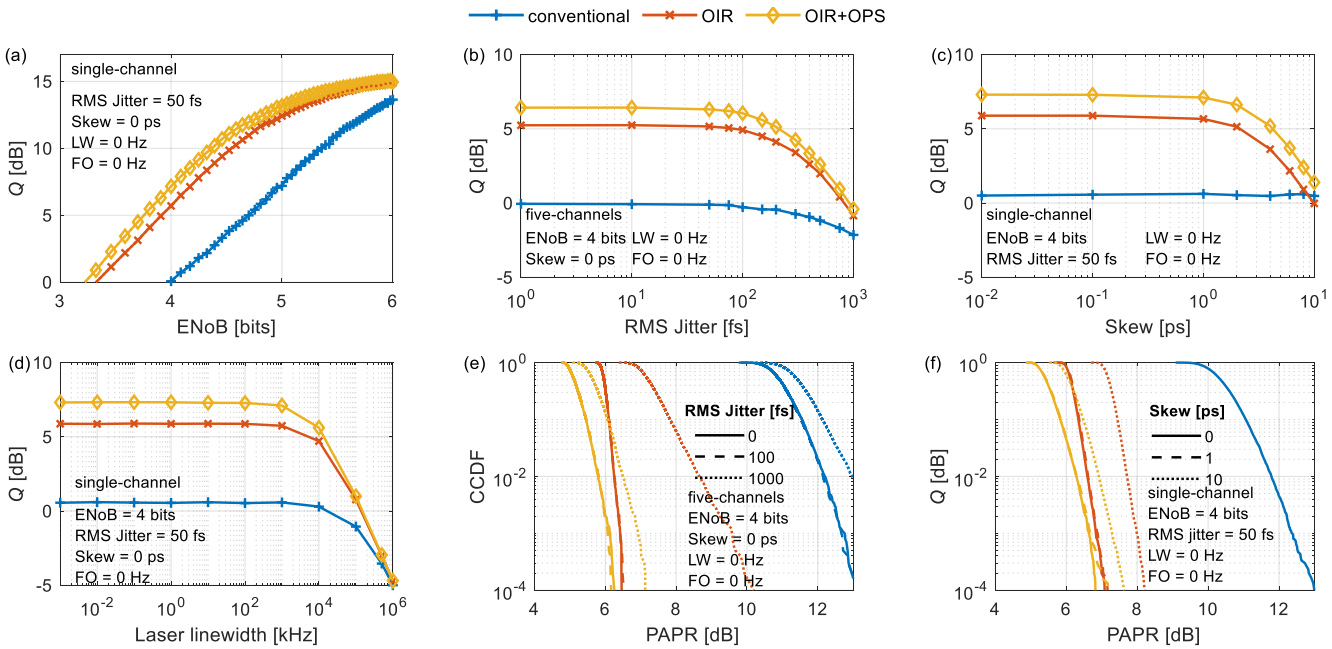

Fig. 6. Transmission performance in a back-to-back configuration with dispersion and noise loading for: (a) Q-factor as a function of ENoB, (b) Q-factor as a function of RMS jitter, (c) Q-factor as a function of skew, (d) Q-factor as a function of laser linewidth, and finally CCDF for PAPR before coherent detection for varying jitter (e) and varying skew (f). In all cases, a single channel was used, except for Fig. 6 (b) and (e) where five channels were considered to match the conditions in Fig. 7. All data points are average over 20 different realizations, with exception of the CCDF plots for which 10000 realizations were used. A time window of 145 ns is considered to evaluate $\max\{|.|^2\}$ in the PAPR.

longer dominant. More importantly, for an ENoB around 4-5 bits, technique OIR allows to achieve a *Q-factor* improvement of 6 dB without OPS and 7.5 with OPS. It should be noted that an improvement of ~6 dB equates to ~1 extra resolution bits. A sensitivity analysis on the RMS jitter is shown in Fig. 6 (b) – Q-factor as a function of RMS jitter. Here we assume the transmission of five WDM channels (in back-to-back). The results show that for Q-factor improvement an RMS jitter smaller than 100 fs is required, and that beyond 1 ps no performance improvement is achieved.

In Fig. 6 (c), the timing alignment requirements are analyzed, assuming no laser phase noise or frequency offset. Here timing alignment refers to the alignment between the measured signal power $|r_{DD}(t)|^2$ and the application of its (processed) multiplicative inverse (i.e., $[filtering(|r_{DD}(t)|^2)]^{-1/2}$) to the optical signal and subsequent digital reconstruction of the coherent optical field (using the DD tap information, i.e., $[filtering(|r_{DD}(t)|^2)]^{1/2}$) – *filtering* relates to the RC-filter described in Section III The impact of time misalignment/skew on the performance of all techniques is shown in Fig. 6 (c). In this figure, performance for the proposed technique starts degrading for a skew larger than 1 ps. Note that the skew targets in conventional receivers, lower than 1 ps [32], covers the requirements for the technique proposed here.

The laser phase noise requirements are analyzed in Fig. 6 (d). The figure shows Q-factor as a function of the laser linewidth, assuming the transmitter and receiver lasers have the same linewidth and uncorrelated phase noise. In can be seen that, for the OIR technique performance starts degrading beyond 100 kHz – although initially with a shallow slope as performance is limited by the mismatch between the ENoB and the constellation cardinality. For arbitrarily large laser linewidth, the performance of OIR and conventional receivers match, indicating the OIR technique imposes negligible additional laser linewidth requirements.

The impact of frequency offset has also been analyzed but it is omitted here since the impact follows that seen in Fig. 6 (d) for laser linewidth. Given the same ADC characteristics, ENoB, bandwidth and jitter, OIR requirements on frequency offset approach that of the conventional receiver. This can be understood noting that the intensity reshaping process is based on optical direct detection before the optical 90 hybrid.

As previously mentioned, OIR tries to improve ENoB by reducing the signal PAPR. Fig. 6 (e) investigates how the cumulative distribution function (CCDF) of PAPR (after coherent detection, but before the quad set of ADCs) is affected by the RMS jitter for the scenarios with the conventional receiver and those implementing OIR, with and without OPS. Note that the results in Fig. 6 (e) were conducted in a WDM scenario with five channels, but neglecting laser phase noise and frequency offset. These conditions match those of Fig. 6 (b). Also, note that the same RMS jitter is considered for all the DACs/ADCs in the schemes analyzed – leading to a PAPR increase with RMS jitter also for conventional receiver (Fig. 6 (e)) since a timing jitter gives rise to signal distortion and an effective amplitude jitter [28]. The results in Fig. 6 (e) show no impact of an RMS jitter of 100 fs (dashed lines) on the PAPR reductions achieved by OIR with and without OPS. And that OIR provided at least 5 dB reduction of PAPR. Due to the additional intensity stripping, further reductions are observed when combining OIR and OPS, reaching values around 6 dB. Increasing the RMS jitter to 1 ps (dotted lines) had a similar impact on both the PAPR given a conventional transmitter and receiver pair and on the PAPR with a conventional transmitter and an OIR+OPS receiver – this level of degradation is likely to be caused solely by DAC amplitude errors given the jitter. On the other hand, the PAPR reduction given a OIR receiver

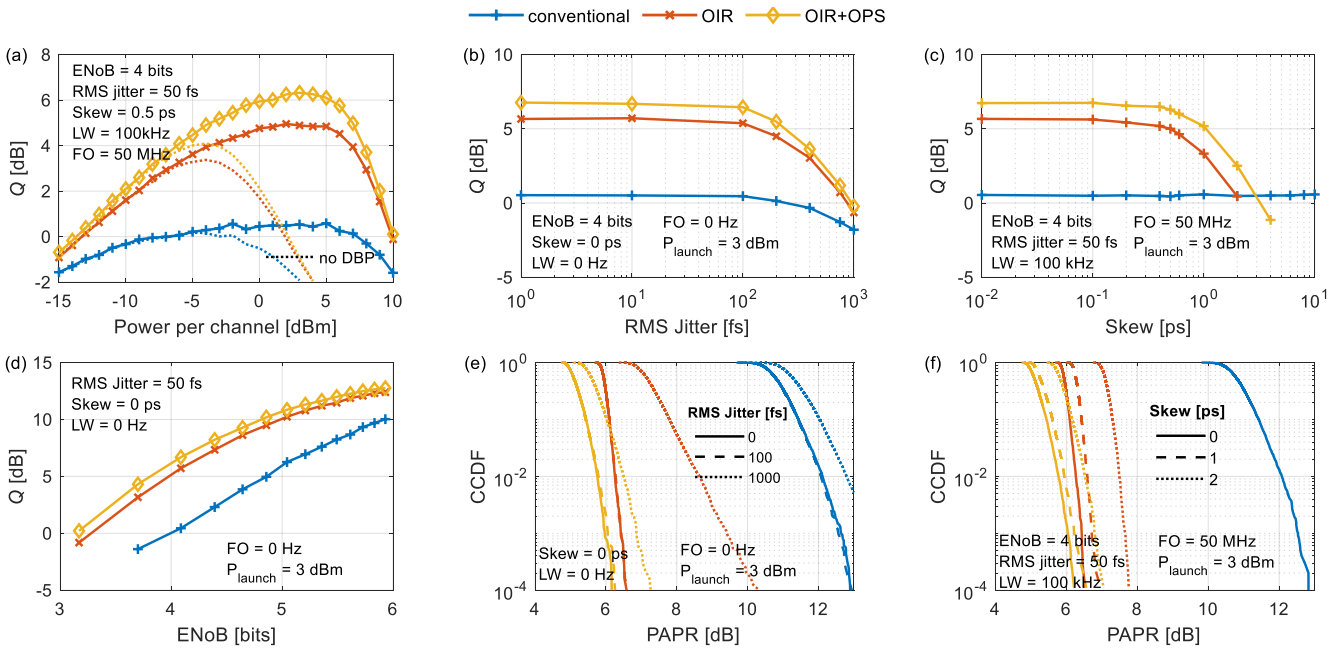

Fig. 7. Transmission performance after 6 spans of 20km: (a) Q-factor as a function of the *launch power* with and without DBP, (b) Q-factor as a function of RMS jitter, (c) Q-factor as a function of skew, (d) Q-factor as a function of the ENoB, and finally CCDF for PAPR before coherent detection for varying jitter (e) and varying skew (f). All data points are average over 40 different realizations, with exception of the CCDF plots (e) and (f) for which 30000 realizations were used per configuration.

(without OPS) was more affected – note that in this case DAC/ADC jitter impact is compounded by using only one direct detection tap for the OIR receiver. Finally, comparing Figs. 6 (b) and 6 (e), one can observe that the PAPR reduction obtained even at relatively large RMS jitter values (1 ps), does not translate into Q-factor gains. This happens due to the impact of RMS jitter on the signal reconstruction.

Fig. 6 (f) shows an analysis of the CCDF of PAPR (after coherent detection, but before the quad set of ADCs) at the presence of different time misalignment/skew conditions. The results show no PAPR degradation for a skew of 1 ps (dashed lines) – in line with the Q-factor results in Fig. 6 (c). Although a significant PAPR improvement is still available for a skew of 10 ps, it does not translate into a Q-factor when looking at Fig. 6 (c) – due to the impact of skew on the signal reconstruction after digitization.

B. Multi-span transmission

In the following, we further evaluate the performance of the proposed method considering transmission over 6 spans of 20 km as a function of the launching power for ENoB = 4 bits, RMS jitter = 50 fs, skew = 0.5ps, laser linewidth LW = 100 kHz, and frequency offset FO = 50 MHz. Here we consider short spans to operate in a regime limited by nonlinear distortion and because, as shown in [33], the required energy per bit is minimized for span lengths going from 35 km at 6 bits/s/Hz to 20 km at 12 bits/s/Hz. With a total WDM bandwidth of 145 GHz, the center WDM channel will experience Kerr nonlinear interactions with the neighboring channels in optical fibers. For such a scenario, we want to demonstrate how the extra ENoB at the coherent receiver improves the performance of DBP. Full-band DBP is implemented following a SSFM method implementation with a 100-m step and no PMD. Note that forward propagation also considered SSFM but with a step bounded by the local error method [30] below 10^{-5} and a PMD of 0.04 ps/√km. Full-band DBP is implemented after simultaneous demultiplexing and detecting a WDM super-channel (with a bandwidth limitation equal to *N*-channels times the channel spacing) – 145GHz for 5-channels. The focus here is not on DBP computational efficiency but on the ultimate performance gains delivered by the ENoB enhancement methods proposed.

Fig. 7 (a) shows the Q-factor for the method OIR with and without OPS as a function of launch power. The results refer to the cases with (full lines) and without (dashed lines) DBP. From Fig. 7 (a) it can be seen that for the non-DBP cases, a gain of ~4 dB is achievable with OIR at optimum launch power. This Q-factor improvement, although significant, is smaller than those in Fig. 6 mainly because the *linear OSNR* has been decreased due to the noise figure of the optical link, and because of the nonlinear distortion, which sets the optimum launch power at around -5 dBm. However, when applying DBP in combination with OIR a significant mitigation of the nonlinear noise translates into additional gains. At optimum launch power, a gain of 6 dB can be observed for OIR+OPS. Hereafter, all the analysis considers the use of DBP and transmission at the optimal launch power of 3 dBm.

The analysis of the RMS jitter impact on the technique OIR is shown in Fig. 7 (b). All the other impairments were neglected here. The results are comparable to those shown in Fig. 6 (b) for the back-to-back configuration. Assuming RMS jitter, frequency offset and laser phase noise, Fig. 7 (c) assesses the effects of skew on the Q-factor obtained with OIR. One can observe that the Q-factor gains provided by OIR with and without OPS start to reduce earlier than observed at the back-to-back scenario shown in Fig. 6 (c) – this is related only to the fact that Fig. 7 (c) considers detection of five WDM channels as opposed to single-channel in Fig. 6 (c). However, for OIR+OPS the Q-factor gains are still above 5 dB for a skew around 1 ps.

Fig. 7 (d) shows Q-factor as a function of ADCs ENoB. The performance gains are larger for ENoB between 3.5 and 4.5 bits, while starting to saturate for ENoB > 5 bits. Note that Q-factor gain reduces at high ENoB once the quantization noise is no longer dominant, as observed in Fig. 6 (a). Finally, Fig. 7 (e) and Fig. 7 (f) investigate the CCDF of PAPR for different levels of RMS jitter and skew, respectively. In both cases, the results are comparable to those obtained in back-to-back configurations when considering the detection of the same number of WDM channels, demonstrating that OIR is reliable also for multi-span transmission – despite the added fiber's nonlinearities and PMD as well as laser impairments (in Fig. 7 (f)). Note that the results for the back-to-back configuration were obtained with a loaded (accumulated) chromatic dispersion of 17 μm/nm, which ultimately led to the CCDFs being similar for both investigated scenarios – otherwise, PAPR would initially increase with distance and the accumulated dispersion [34] until it would saturate [35, 36].

From the results above, the technique OIR leads to additional performance when compared to conventional receivers. Additionally, the extra components required, including the scenario with OPS, can be readily integrated in the existing coherent receiver architecture. These characteristics make OIR+OPS a technique suitable for practical implementation, with performance gains potentially compatible with the complexity of changing and adding it to the standard optical coherent receiver front-end.

V. Conclusion

We explore a novel optical signal processing and optoelectronic technique to enhance the effective vertical resolution of coherent optical receivers through optical intensity reshaping. With this technique, one can exploit the benefits of linearity, broadband and low noise of optical passive operations and optoelectronic mixers.

Investigations have been conducted both in the linear and nonlinear power regimes, assuming a realistic ADC/DAC model with bandwidth limitations including jitter, also assessing performance when applying nonlinear digital compensation. Assuming single channel transmission over a linear channel, the Q-factor results showed improvements of as much as 7 dB for the technique OIR, for ADCs with ENoB of 4 bits and an RMS jitter of 50 fs. Note that these gains approach and surpass those that would be obtained by adding one extra *effective* bit to the ADC array in a standard coherent receiver. For WDM transmission, gains of ~4 dB were observed by using OIR combined with OPS. When performing full-band DBP, additional gains were observed for the scenarios investigated reaching 6 dB. The results showed that the techniques OIR can be used to enhance effective vertical resolution, possibly alleviating requirements in terms of ENoB of ADCs. In particular, the OIR technique has potential for practical implementation requiring only one extra ADC.

Finally, the additional ENoB boost offered by the technique proposed and analyzed here can be used in two different ways, either by keep operating at the same bandwidth and benefiting of the additional SNR offered by the additional ENoB, or by selecting an ADC set with lower ENoB but larger electronic bandwidth. Increasing the bandwidth would be a more effective way to increase the bit rate and share the cost and power-consumption of optoelectronic components across many bits.

References

[1] C. Laperle and M. O'Sullivan, "Advances in High-Speed DACs, ADCs, and DSP for Optical Coherent Transceivers," *Journal of Lightwave Technology*, vol. 32, no. 4, pp. 629-643, 2014, doi: 10.1109/JLT.2013.2284134.

[2] A. Erik *et al.*, "Roadmap of optical communications," *Journal of Optics*, vol. 18, no. 6, p. 063002, 2016. [Online]. Available: http://stacks.iop.org/2040-8986/18/i=6/a=063002.

[3] R. H. Walden, "Analog-to-Digital Converters and Associated IC Technologies," in *2008 IEEE Compound Semiconductor Integrated Circuits Symposium*, 12-15 Oct. 2008 2008, pp. 1-2, doi: 10.1109/CSICS.2008.43.

[4] P. J. Winzer, "The future of communications is massively parallel," *Journal of Optical Communications and Networking*, vol. 15, no. 10, pp. 783-787, 2023/10/01 2023, doi: 10.1364/JOCN.496992.

[5] T. Pfau, S. Hoffmann, and R. Noe, "Hardware-Efficient Coherent Digital Receiver Concept With Feedforward Carrier Recovery for <formula formulatype="inline"><tex Notation="TeX">M</tex></formula>-QAM Constellations," *Journal of Lightwave Technology*, vol. 27, no. 8, pp. 989-999, 2009, doi: 10.1109/JLT.2008.2010511.

[6] X. Chen, S. Chandrasekhar, S. Randel, W. Gu, and P. Winzer, "Experimental quantification of implementation penalties from limited ADC resolution for Nyquist shaped higher-order QAM," in *2016 Optical Fiber Communications Conference and Exhibition (OFC)*, 20-24 March 2016 2016, pp. 1-3.

[7] S. Beppu, K. Kasai, M. Yoshida, and M. Nakazawa, "2048 QAM (66 Gbit/s) single-carrier coherent optical transmission over 150 km with a potential SE of 15.3 bit/s/Hz," *Optics Express*, vol. 23, no. 4, pp. 4960-4969, 2015/02/23 2015, doi: 10.1364/OE.23.004960.

[8] S. Okamoto, M. Terayama, M. Yoshida, K. Kasai, T. Hirooka, and M. Nakazawa, "Experimental and numerical comparison of probabilistically shaped 4096 QAM and a uniformly shaped 1024 QAM in all-Raman amplified 160 km transmission," *Optics Express*, vol. 26, no. 3, pp. 3535-3543, 2018/02/05 2018, doi: 10.1364/OE.26.003535.

[9] E. Sillekens, G. Liga, D. Lavery, P. Bayvel, and R. I. Killey, "High-Cardinality Geometrical Constellation Shaping for the Nonlinear Fibre Channel," *Journal of Lightwave Technology*, vol. 40, no. 19, pp. 6374-6387, 2022, doi: 10.1109/JLT.2022.3197366.

[10] Y. Wakayama *et al.*, "2048-QAM transmission at 15 GBd over 100 km using geometric constellation shaping," *Optics Express*, vol. 29, no. 12, pp. 18743-18759, 2021/06/07 2021, doi: 10.1364/OE.423361.

[11] W. Kester, "MT-001 TUTORIAL Taking the Mystery out of the Infamous Formula , " SNR = 6 . 02 N + 1 . 76 dB , " and Why You Should Care by," 2009.

[12] P. J. Winzer and D. T. Neilson, "From Scaling Disparities to Integrated Parallelism: A Decathlon for a Decade," *Journal of Lightwave Technology*, vol. 35, no. 5, pp. 1099-1115, 2017, doi: 10.1109/JLT.2017.2662082.

[13] E. Ip, A. P. T. Lau, D. J. F. Barros, and J. M. Kahn, "Coherent detection in optical fiber systems," *Optics Express*, vol. 16, no. 2, pp. 753-791, 2008/01/21 2008, doi: 10.1364/OE.16.000753.

[14] L. Galdino *et al.*, "On the limits of digital back-propagation in the presence of transceiver noise," *Optics Express*, vol. 25, no. 4, pp. 4564-4578, 2017/02/20 2017, doi: 10.1364/OE.25.004564.

[15] P. Bayvel *et al.*, "Maximizing the optical network capacity," *Philosophical transactions. Series A, Mathematical, physical, and engineering sciences*, vol. 374, 2016.

[16] R. Maher, A. Alvarado, D. Lavery, and P. Bayvel, "Increasing the information rates of optical communications via coded modulation: a study of transceiver performance," *Scientific Reports*, Article vol. 6, p. 21278, 02/11/online 2016, doi: 10.1038/srep21278.

[17] E. Ip and J. M. Kahn, "Compensation of Dispersion and Nonlinear Impairments Using Digital Backpropagation," *Journal of Lightwave Technology*, vol. 26, no. 20, pp. 3416-3425, 2008, doi: 10.1109/JLT.2008.927791.

[18] J. Cho and P. J. Winzer, "Probabilistic Constellation Shaping for Optical Fiber Communications," *Journal of Lightwave Technology*,

vol. 37, no. 6, pp. 1590-1607, 2019, doi: 10.1109/JLT.2019.2898855.

[19] F. Buchali, F. Steiner, G. Böcherer, L. Schmalen, P. Schulte, and W. Idler, "Rate Adaptation and Reach Increase by Probabilistically Shaped 64-QAM: An Experimental Demonstration," *Journal of Lightwave Technology*, vol. 34, no. 7, pp. 1599-1609, 2016, doi: 10.1109/JLT.2015.2510034.

[20] B. Chen, Y. Lei, D. Lavery, C. Okonkwo, and A. Alvarado, "Rate-Adaptive Coded Modulation with Geometrically-shaped Constellations," in *2018 Asia Communications and Photonics Conference (ACP)*, 26-29 Oct. 2018 2018, pp. 1-3, doi: 10.1109/ACP.2018.8595918.

[21] E. Agrell and M. Karlsson, "Satellite constellations: Towards the nonlinear channel capacity," in *IEEE Photonics Conference 2012*, 23-27 Sept. 2012 2012, pp. 316-317, doi: 10.1109/IPCon.2012.6358619.

[22] Q. Zhang and C. Shu, "Constellation size for probabilistic shaping under the constraint of limited ADC resolution," *Opt. Lett.*, vol. 44, no. 23, pp. 5820-5823, 2019/12/01 2019, doi: 10.1364/OL.44.005820.

[23] E. Ip *et al.*, "Optimization of Probabilistic Shaping Enabled Transceivers with Large Constellation Sizes for High Capacity Transmission," in *2018 European Conference on Optical Communication (ECOC)*, 23-27 Sept. 2018 2018, pp. 1-3, doi: 10.1109/ECOC.2018.8535393.

[24] A. E. Willner, S. Khaleghi, M. R. Chitgarha, and O. F. Yilmaz, "All-Optical Signal Processing," *Journal of Lightwave Technology*, vol. 32, no. 4, pp. 660-680, 2014/02/15 2014. [Online]. Available: http://jlt.osa.org/abstract.cfm?URI=jlt-32-4-660.

[25] R. P. Webb, J. M. Dailey, R. J. Manning, and A. D. Ellis, "Phase discrimination and simultaneous frequency conversion of the orthogonal components of an optical signal by four-wave mixing in an SOA," *Optics Express*, vol. 19, no. 21, pp. 20015-20022, 2011/10/10 2011, doi: 10.1364/OE.19.020015.

[26] Josuke Ozaki, Yoshihiro Ogiso, and S. Nakano, "High-speed Modulator for Next-generation Large-capacity Coherent Optical Networks," *NTT Technical Review*, vol. 16, no. 4, pp. 49-56, 2018.

[27] B. Geiger, E. Sillekens, F. Ferreira, R. Killey, L. Galdino, and P. Bayvel, "On the Performance Limits of High-Speed Transmission Using a Single Wideband Coherent Receiver," *Journal of Lightwave Technology*, vol. 41, no. 12, pp. 3816-3824, 2023, doi: 10.1109/JLT.2023.3277624.

[28] S. Varughese, J. Langston, V. A. Thomas, S. Tibuleac, and S. E. Ralph, "Frequency Dependent ENoB Requirements for M-QAM Optical Links: An Analysis Using an Improved Digital to Analog Converter Model," *Journal of Lightwave Technology*, vol. 36, no. 18, pp. 4082-4089, 2018, doi: 10.1109/JLT.2018.2859637.

[29] S. Varughese, D. Lippiatt, S. Tibuleac, and S. E. Ralph, "Frequency Dependent ENoB Requirements for 400G/600G/800G Optical Links," *Journal of Lightwave Technology*, vol. 38, no. 18, pp. 5008-5016, 2020, doi: 10.1109/JLT.2020.3000177.

[30] O. V. Sinkin, R. Holzlohner, J. Zweck, and C. R. Menyuk, "Optimization of the split-step fourier method in modeling optical-fiber communications systems," *J. Light. Technol.*, vol. 21, no. 1, pp. 61-68, 2003, doi: 10.1109/jlt.2003.808628.

[31] R. Schmogrow *et al.*, "Error Vector Magnitude as a Performance Measure for Advanced Modulation Formats," *IEEE Photonics Technology Letters*, vol. 24, no. 1, pp. 61-63, 2012, doi: 10.1109/LPT.2011.2172405.

[32] *Implementation Agreement for Integrated Coherent TransmitReceive Optical Sub Assembly*, IA # OIF-IC-TROSA-01.0, OIF, 2019.

[33] N. J. Doran and A. D. Ellis, "Minimising total energy requirements in amplified links by optimising amplifier spacing," *Optics Express*, vol. 22, no. 16, pp. 19810-19817, 2014/08/11 2014, doi: 10.1364/OE.22.019810.

[34] K. Roberts *et al.*, "Performance of Dual-Polarization QPSK for Optical Transport Systems," *Journal of Lightwave Technology*, vol. 27, no. 16, pp. 3546-3559, 2009, doi: 10.1109/JLT.2009.2022484.

[35] Y. Yoshida, A. Maruta, and K. i. Kitayama, "On the peak-to-average power ratio distribution along fiber in the optical OFDM transmissions," in *2011 37th European Conference and Exhibition on Optical Communication*, 18-22 Sept. 2011 2011, pp. 1-3.

[36] C. Xie, "Chromatic Dispersion Estimation for Single-Carrier Coherent Optical Communications," *IEEE Photonics Technology Letters*, vol. 25, no. 10, pp. 992-995, 2013, doi: 10.1109/LPT.2013.2257729.